

# Experimental fission study using multi-nucleon transfer reactions

Katsuhisa Nishio<sup>1,a</sup>, Kentaro Hirose<sup>1</sup>, Romain L guillon<sup>1</sup>, Hiroyuki Makii<sup>1</sup>, Riccardo Orlandi<sup>1</sup>, Kazuaki Tsukada<sup>1</sup>, James Smallcombe<sup>1,2</sup>, Satoshi Chiba<sup>3</sup>, Yoshihiro Aritomo<sup>4</sup>, Shouya Tanaka<sup>4</sup>, Tsutomu Ohtsuki<sup>5</sup>, Igor Tsekhanovich<sup>6</sup>, Costel M. Petrache<sup>7</sup>, and Andrei Andreyev<sup>8,1</sup>

<sup>1</sup> Advanced Science Research Center, Japan Atomic Energy Agency, 2-4 Shirakata, Tokai, Naka-gun, Ibaraki 319-1195, Japan

<sup>2</sup> TRIUMF, Vancouver, British Columbia V6T 2A3, Canada

<sup>3</sup> Laboratory for Advanced Nuclear Energy, Tokyo Institute of Technology, 2-12-1, Ookayama, Meguro-ku, Tokyo 152-8550, Japan

<sup>4</sup> Faculty of Science and Engineering, Kindai University, Higashi-Osaka 577-8502, Japan

<sup>5</sup> Research Reactor Institute, Kyoto University, Kumatori-cho, Sennangun, Osaka 590-0494, Japan

<sup>6</sup> Universit  de Bordeaux, 351 Cours de la Lib ration, 33405 Talence Cedex, France

<sup>7</sup> Centre des Sciences Nucl aire et des Sciences de la Mati re, Universit  Paris-Saclay, CNRS/IN2P3, 91406 Orsay, France

<sup>8</sup> Department of Physics, University of York, Heslington, York, YO10 5DD, UK

**Abstract.** It is shown that the multi-nucleon transfer reactions is a powerful tool to study fission of exotic neutron-rich actinide nuclei, which cannot be accessed by particle-capture or heavy-ion fusion reactions. In this work, multi-nucleon transfer channels of the reactions of  $^{18}\text{O}+^{232}\text{Th}$ ,  $^{18}\text{O}+^{238}\text{U}$  and  $^{18}\text{O}+^{248}\text{Cm}$  are used to study fission for various nuclei from many excited states. Identification of fissioning nuclei and of their excitation energy is performed on an event-by-event basis, through the measurement of outgoing ejectile particle in coincidence with fission fragments. Fission fragment mass distributions are measured for each transfer channel. Predominantly asymmetric fission is observed at low excitation energies for all studied cases, with a gradual increase of the symmetric mode towards higher excitation energy. The experimental distributions are found to be in general agreement with predictions of the fluctuation-dissipation model. Role of multi-chance fission in fission fragment mass distributions is discussed, where it is shown that mass-asymmetric structure remaining at high excitation energies originates from low-excited nuclei by evaporation of neutrons.

## 1. Introduction

Nuclear fission, discovered more than 75 years before, still remains as a challenging subject in nuclear physics as an unique phenomenon observed in nuclear matter. The process is largely influenced by the internal shell structures appearing in the deformed nuclear shape, and thus have information on single-particle levels in an extreme shape of massive nuclei. Also dynamical effects should be introduced to explain various aspects in fission. New experimental techniques and associated new data are indispensable to further understand fission mechanism. Fission-fragment mass distributions (FFMDs) are one of the most fundamental data. Neutron- and charged particle capture reactions have been used to populate low-excited compound nuclei for fission study [1,2]. Spontaneous fission, starting from ground state, is the extreme case in low energy fission. Around 2000 GSI developed a Coulex-induced fission of relativistic RIBs in inverse kinematics, comprehensive fission studies were performed for several tens of nuclei in the neutron-deficient Ac-U region [3]. The recent SOFIA experiment at GSI also followed the same approach but with a much improved technique [4]. Recently,  $\beta$ /EC delayed fission was investigated for the

very proton-rich nucleus using radioactive beams, and  $^{180}\text{Hg}$  was found to show an asymmetric fission as a new region of mass-asymmetric fission [5].

Multi-nucleon transfer (MNT) reactions is another unique reaction which allow us to populate neutron-rich nuclei which cannot be accessed by other reactions such as particle capture and/or heavy-ion fusion reactions. Furthermore, in the MNT reaction excited states of compound nuclei (CN) range widely from under the fission barrier to higher energies, allowing us to measure the excitation energy dependence of FFMDs. From the threshold excitation energy over which fission takes place, fission-barrier height can be derived. The MNT reactions are further used for a surrogate reaction technique as a method to determine the neutron-induced fission cross sections [6]. Recently, an inverse kinematics technique was used in the MNT channels of the  $^{238}\text{U}+^{12}\text{C}$  reaction, to study fusion-fission of excited transactinide nuclei with the help of the large-acceptance magnetic spectrometer VAMOS@GANIL [7–9]. In these experiments, sufficiently-high  $A$  and  $Z$  resolution for FFs was achieved due to their kinematic boost, allowing the simultaneous measurement of the complete mass- and atomic-number distributions of fission fragments.

At the tandem accelerator facility of the Japan Atomic Energy Agency (JAEA), we studied the MNT channels of

<sup>a</sup> e-mail: nishio.katsuhisa@jaea.go.jp

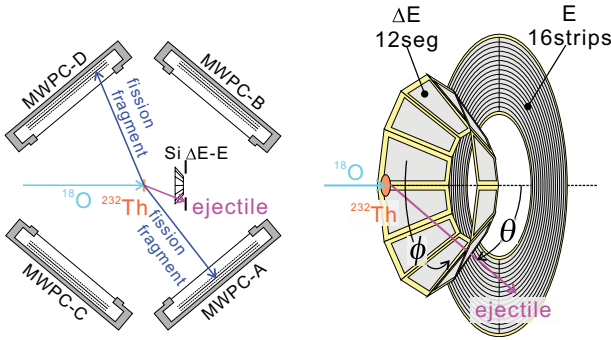


**Figure 1.** Schematic detection set-up (left) and expanded view of the silicon  $\Delta E$ -E detector telescope (right). See text for details.

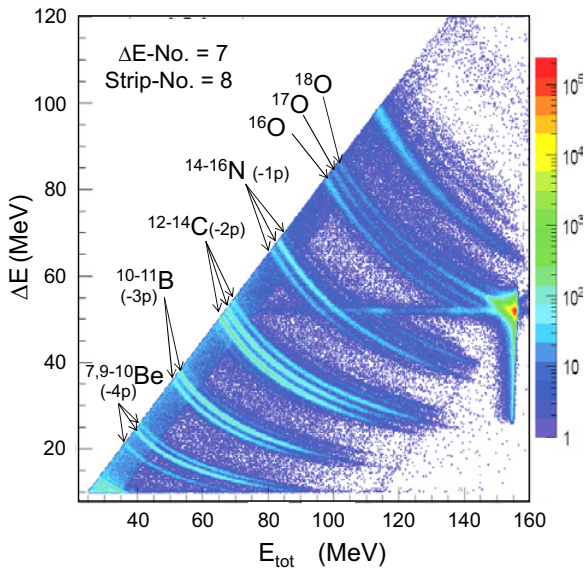


**Figure 2.**  $\Delta E$ - $E_{tot}$  spectrum for ejectiles measured by one pair of the  $\Delta E$ -E detectors obtained in the  $^{18}\text{O}+^{232}\text{Th}$  reaction [10]. The curves corresponding to different ejectiles are marked with the respective isotopes. The scattered  $^{18}\text{O}$  is also seen in the plot.

the reaction  $^{18}\text{O}+^{232}\text{Th}, ^{238}\text{U}, ^{248}\text{Cm}$  in direct kinematics to obtain FFMDs and their excitation-energy dependence for various isotopes (Data for  $^{18}\text{O}+^{232}\text{Th}$  was published in [10]). An obvious advantage of this method is a relatively easy possibility to change the projectile and/or the target nuclei. In particular by using targets of the rarest highly-radioactive neutron-rich isotopes heavier than  $^{238}\text{U}$  (e.g., Cm and Cf), nuclei to be studied can be extended to isotopes far heavier than uranium, which cannot be used at the accelerator facilities for the inverse kinematics experiments similar to VAMOS or SOFIA.

## 2. Experimental methods

An  $^{18}\text{O}$  beam was supplied by the JAEA-tandem accelerator at a typical beam intensity of about  $0.5 \text{ p nA}$ . Beam energies were 157–162 MeV, depending on the different run. Targets were prepared by electrodeposition of oxide-target material on a Ni backing of about  $90 \mu\text{g}/\text{cm}^2$  thickness. Thickness of the target-material layer was 30–148  $\mu\text{g}/\text{cm}^2$ .

For the event-by-event identification of the transfer channel (thus, of the fissioning nucleus) and of respective coincident FFs, a detection system consisting of a  $\Delta E$ -E silicon detector telescope and four multiwire proportional chambers (MWPC) were used, see Fig. 1. Specific transfer channels were identified by detecting projectile-like (ejectile) nuclei in twelve  $75 \mu\text{m}$ -thick trapezoidal  $\Delta E$  silicon detectors which were mounted in a cone around the beam axis, each with the azimuthal angle acceptance of  $\Delta\phi = 22.5^\circ$ . After passing through the  $\Delta E$  detector, the ejectiles impinged on the  $300 \mu\text{m}$ -thick annular silicon strip detector (E-detector), divided in 16 annular strips, which allows determination of the scattering angle  $\theta$ . The inner and outer radius of the detector are 24.0 mm and 48.0 mm, respectively, corresponding to the acceptance angle  $\theta$  between  $16.7^\circ$  and  $31.0^\circ$  relative to the beam direction.

The energy calibration of the E-detectors was performed by removing two  $\Delta E$ -detectors so that the elastically-scattered  $^{18}\text{O}$  beam could hit the E-detector directly. The well-defined initial beam energy from the tandem and the measured scattering energy  $E_{\text{elastic}}(\theta)$  (as a function of the scattering angle) were then used to calibrate the strips of the E-detector. Elastic scattering was further used to calibrate the  $\Delta E$ -detectors, by determining the energy deposition in the  $\Delta E$ -detector as  $E_{\text{elastic}} - E_{\text{res}}$ , where  $E_{\text{res}}$  is the energy measured in the E-detector after passing through the  $\Delta E$ -detector. From the peak of elastic scattering in the sum spectrum  $E_{\text{tot}} = \Delta E + E_{\text{res}}$ , the energy resolution was obtained to be 0.9–1.0 MeV (FWHM), which also determines the precision for the excitation energies deduced in our study.

Figure 2 shows the  $\Delta E$ - $E_{\text{tot}}$  spectrum for ejectiles obtained in the  $^{18}\text{O}+^{232}\text{Th}$  reaction, where the parabolic lines correspond to different transfer channels, including a clear separation of specific isotopes. Isotopic assignment was done in respect of the elastically-scattered peak of  $^{18}\text{O}$  and the missing line of  $^8\text{Be}$ . It was further confirmed with the energy-loss calculation using the program SRIM [11]. The identification of the  $^{12}\text{C}$  line was also checked by accelerating a  $^{12}\text{C}$  beam and measuring the elastic peak. The data from  $\Delta E$ -E spectra were also used to deduce the excitation energy of the respective fissioning nuclei, which were determined from reaction Q-value [12] and the measured (angle-dependent) ejectile energies  $\Delta E$  and  $E_{\text{tot}}$ . In this procedure we assumed that no excitation energy is given to the ejectile, thus the excitation energies quoted should be considered as upper limits only. Though the precision of the deduced excitation energies is  $\sim 1 \text{ MeV}$  and the obtained statistics in the experiments, excitation-energy range of 10 MeV was chosen as a bin to draw the evolution of the FFMDs with excitation energy.

The coincident FFs resulting from the fission of excited nuclei after the MNT reaction are detected by four  $200 \times 200 \text{ mm}^2$  position-sensitive MWPCs, see in Fig. 1. The MWPCs were operated with an isobutane gas of about 1.5 Torr [13]. The distance between the target and the center of the cathode was 224 mm, and each MWPC covers a solid angle of 0.67 sr. The positions of FFs's incidence on the MWPC were determined with a position resolution of 4.0 mm. Charge induced in the cathode of the MWPC was recorded to separate fission fragment and other reaction products. Typical rise time of the MWPC is 5 ns. Both fission fragments were detected in coincidence

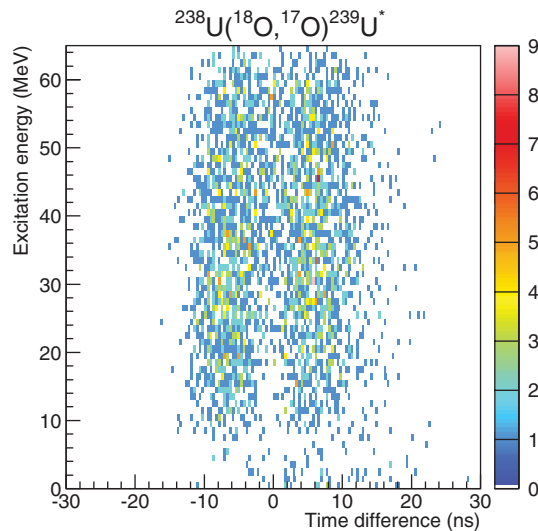


**Figure 3.** Fission events recorded on the time difference between the signals from coincided MWPCs and excitation energy obtained in one neutron transfer reaction  $^{238}\text{U}(^{18}\text{O}, ^{17}\text{O})^{239}\text{U}^*$ .

with a pair of MWPC facing on both side of the target,  $(+50.1^\circ, -129.9^\circ)$  or  $(-50.1^\circ, +129.9^\circ)$  relative to the beam direction. FF time differences,  $\Delta T$ , between two coincident MWPCs were measured to determine the masses of both fragments. Figure 3 shows an example of recorded fission fragments on the time difference and excitation energy in the transfer channel of  $^{18}\text{O}+^{238}\text{U} \rightarrow ^{19}\text{O}+^{239}\text{U}^*$ . Two regions are clearly observed in the low-excitation fissions, corresponding to the light- and heavy-fragment groups, which however smears for the events at high-excitation energies.

### 3. Results

FFs masses were determined event-by-event from the kinematic analysis, where the measured  $\Delta T$  values and incident positions of both FFs were used. The momentum of the target-like fissioning recoil nucleus is determined by the measured momentum of ejectile under the assumption of a binary reaction process. To validate the calibration procedure, Fig. 4 shows the comparison of FFMDs for  $^{239}\text{U}^*$ , populated in the  $^{238}\text{U}(^{18}\text{O}, ^{17}\text{O})^{239}\text{U}^*$  reaction, with  $n + ^{238}\text{U}$  [14]. The obtained FFMDs from MNT reactions agree well with the neutron-induced data, particularly mass asymmetry at the peak positions at the lowest energy data and the increase of the symmetric fission with excitation energy are noteworthy. The result demonstrates that  $^{18}\text{O}$ -induced neutron-transfer reaction can be a surrogate of neutron-induced fission to give FFMDs. The FFMDs data for  $^{233}\text{Pa}^*$ ,  $^{233}\text{Th}^*$  and  $^{236}\text{U}^*$  from the MNT reactions of  $^{18}\text{O}+^{232}\text{Th}$  [10] agree with literature data obtained in proton- and neutron-induced fissions [15–18].

Figure 5 shows the FFMDs for nuclei of  $^{231-234}\text{Th}^*$ ,  $^{232-236}\text{Pa}^*$  and  $^{234-238}\text{U}^*$ , populated in the MNT reactions of  $^{18}\text{O} + ^{232}\text{Th}$ . The FFMDs of the  $^{231,234}\text{Th}^*$ ,  $^{234,235,236}\text{Pa}^*$  nuclei were obtained for the first time in this experiment. For the other nuclei, the known FFMD data were systematically extended to excitation energies as high as 60 MeV. It follows from Fig. 5 that mass-asymmetric fission dominates at low excitation energies for all measured nuclei. The yield in the mass-symmetric

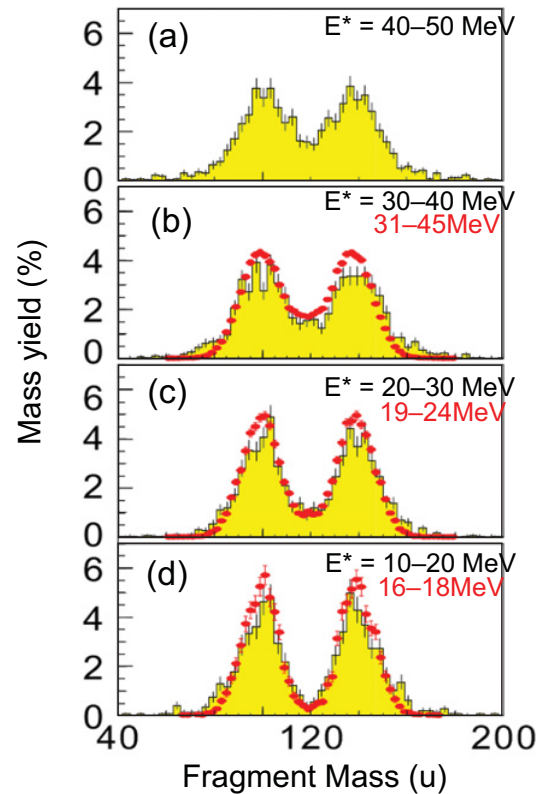


**Figure 4.** Experimental FFMDs (black histogram with error bars) obtained in the  $^{238}\text{U}(^{18}\text{O}, ^{17}\text{O})^{239}\text{U}^*$  reaction. Excitation energy ranges are indicated (black character). Data are compared with those from the  $n+^{238}\text{U}$  [14] from the similar excitation energies (red character).

fission region increases with excitation energy (see also Fig. 4) and the double-humped shapes tend to become structureless due to weakening of shells responsible for asymmetric fission. It is also interesting to note that the measured spectra seem to reveal larger peak-to-valley ratio in the FFMDs for nuclei with larger isospin values, as seen for the most neutron-rich isotopes of the same element, considered at the same excitation energy (see, for instance, FFMDs for  $E^* = 20-40$  MeV). This might be explained by the increasing influence of the magic  $^{132}\text{Sn}$  nucleus on the mass division, which is expected for better matching in the  $N/Z$ -ratios between  $^{132}\text{Sn}$  and the fissioning compound nucleus.

In the results of  $^{18}\text{O}+^{238}\text{U}$ , we obtained the FFMDs for totally 19 nuclei by expanding the analysis of ejectiles of oxygen (uranium compound nuclei), nitrogen (protoactinium), carbon (plutonium), boron (americium), and beryllium (curium) isotopes (see Fig. 2) up to excitation energies as high as 60 MeV [19]. In the  $^{18}\text{O}+^{238}\text{U}$  reactions, new FFMDs data were obtained for nine nuclei of  $^{240}\text{U}^*$ ,  $^{240,241,242}\text{Np}^*$ ,  $^{241,243}\text{Pu}^*$ ,  $^{245,246}\text{Am}^*$ ,  $^{247}\text{Cm}^*$ . In the recent measurement of  $^{18}\text{O}+^{248}\text{Cm}$ , new FFMDs of eleven nuclei are further generated,  $^{247,249}\text{Cm}$ ,  $^{249,250,251,252}\text{Bk}$ ,  $^{251,253}\text{Cf}$ ,  $^{254,256}\text{Es}$ , and  $^{255}\text{Fm}$  [19]. It was found in these experiments that data of low-excited states were not obtained with enough statistics when more than two protons are transferred from the projectile to the target nucleus, due to the small probability to populate low excited states of  $E^* < \sim 20$  MeV.

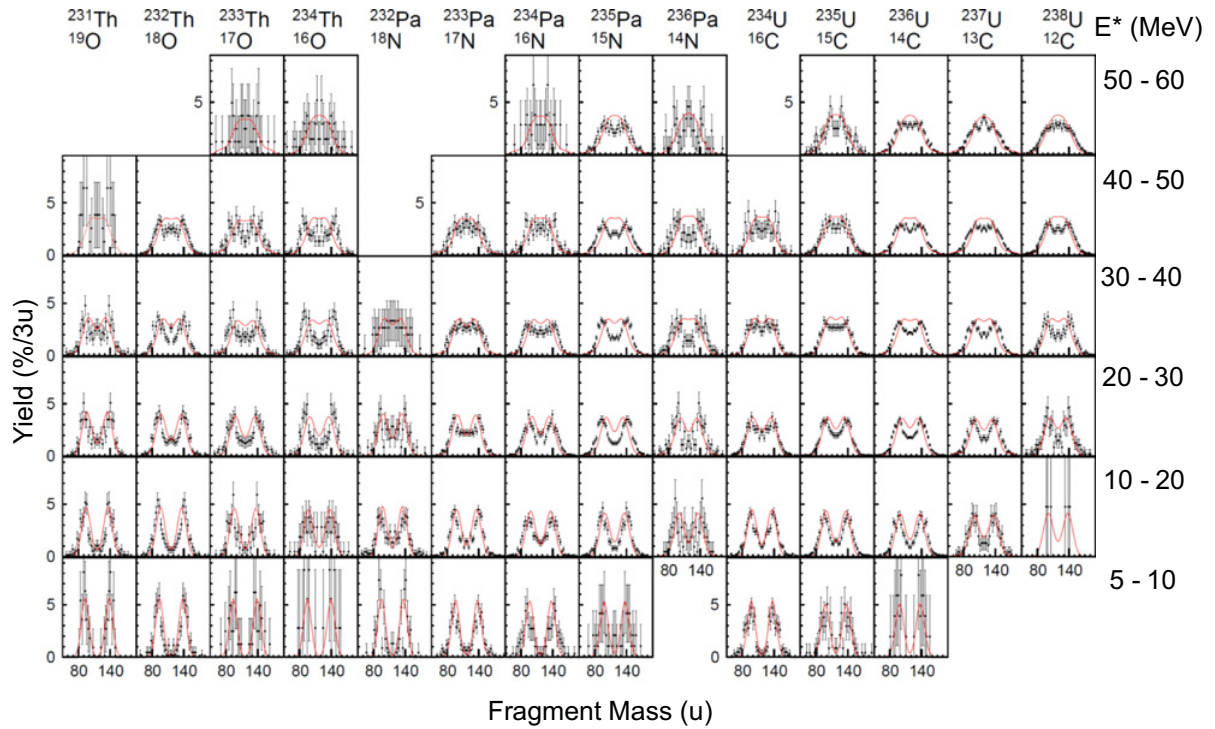


**Figure 5.** FFMDs obtained in the multinucleon transfer channels of the reaction  $^{18}\text{O}+^{232}\text{Th}$  (data points with error bars). The fissioning nucleus and the corresponding ejectile are indicated on the top of the plot. The data are shown for sequential 10 MeV excitation-energy  $E^*$  intervals, indicated on the right side. The red curves are the results of Langevin calculations (see text) [10] after a convolution with the experimental mass resolution, where the initial CN excitation energy is used to start the calculation, but effects of multi-chance fission (neutron evaporation prior to fission) were not included as discussed in the context of Fig. 7.

The evolution of the center of the light- and heavy-fragment groups ( $\bar{A}_L$  and  $\bar{A}_H$ ) with the mass of the CN in low energy fissions of  $10 < E^* < 20$  MeV is shown in Fig. 6, where data were obtained from the three MNT reactions of  $^{18}\text{O}+^{232}\text{Th}$ ,  $^{18}\text{O}+^{238}\text{U}$  and  $^{18}\text{O}+^{248}\text{Cm}$ . It is found that the  $\bar{A}_H$  value are nearly kept constant around 141, whereas center of the light fragment increases linearly with mass of fissioning nucleus. The trend shows the dominant influence of the shell structure in heavy fragments as well-known phenomenon [1]. The present study revealed that number of neutrons contained in the heavy fragments is kept constant through the isotopes in the same element.

#### 4. Discussions

The measured FFMDs from the MNT reactions are compared with calculations based on the fluctuation-dissipation model developed in [20], where description of fission in Langevin equations from the low-excited state was attempted, and a good reproduction of the measured FFMDs for  $^{234,236}\text{U}^*$  and  $^{240}\text{Pu}^*$  from  $E^* = 20$  MeV was obtained. As described in [20], the nuclear shape and the corresponding energy is calculated by a two-center shell model [21]. The nuclear shape is defined by three parameters (distance between two potential centers, deformation of fragments, and mass-asymmetry), and the corresponding energy is given by a sum of the liquid-drop energy  $V_{LD}$  and the shell correction energy  $V_{shell}$ . The latter term is represented as  $V_{shell}(0) \exp(-E^*/E_d)$  using the shell correction energy at the zero temperature  $V_{shell}(0)$  and shell damping parameter  $E_d$ , where  $E_d = 20$  MeV was chosen as in [20]. For simplicity, we assumed that the total

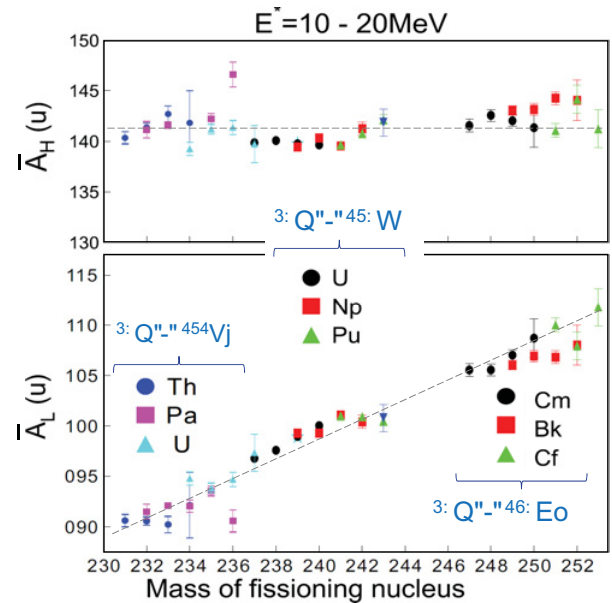


**Figure 6.** Center of the light and heavy fragment groups ( $\bar{A}_L$  and  $\bar{A}_H$ ) as a function of mass of the fissioning nuclei in low-excitation fission of  $10 < E^* < 20$  MeV. Data are obtained from the reactions of  $^{18}\text{O}+^{232}\text{Th}$ ,  $^{238}\text{U}$  and  $^{248}\text{Cm}$  using the same setup shown in Fig. 1.

excitation energy of the system after the MNT reactions is given to the excitation energy ( $E^*$ ) of the fissioning nucleus.

The calculated results are shown in Fig. 5, where the original theoretical curves were broadened with the

experimental resolution. One can see that the calculated FFMDs reproduce reasonably well both the global shape of the experimental distributions and also the positions of the light and heavy-fragment peaks for most of studied nuclides, at the excitation energies below  $\sim 30$  MeV. Furthermore, observation that lighter element (thorium) has a pronounced peak-to-valley ratio than the heavier element (uranium) was also reproduced by the calculation. These agreement demonstrates the reasonable treatment of the shell correction energy at these excitation energies, and confirms the validity of the shell-damping energy of  $E_d = 20$  MeV originally introduced in [22], in contrast to a recently suggested value of  $E_d = 60$  MeV [23].

However, significant deviations of the calculation in Fig. 5 are recognized, especially at higher excitation energies. For example, calculated spectra at  $E^* = 30$ – $40$  MeV and higher energies show a tendency to favor the symmetric fission mode for most of the studied nuclei, whereas experimentally several nuclei still exhibit a clear mass asymmetry especially for the most neutron-rich isotopes (for example  $^{234}\text{Th}^*$ ,  $^{236}\text{Pa}^*$ ,  $^{238}\text{U}^*$ ). This can be interpreted as the effects of multi-chance fission that excited compound nucleus emits neutrons prior to fission. With increasing the excitation energy, the contribution from multi-chance fission becomes increasingly important. Thus, the fission observable, in particular FFMDs, become a superposition of several contributions, originating from fission at different excitation energies. These features are demonstrated by Fig. 7, which compares the experimental data for fission of  $^{238}\text{U}^*$  at the initial excitation energy  $E^* = 35$  MeV with the Langevin calculation taking into account multi-chance fission. According to calculations, at this initial energy, the 1st- and 2nd-chance fission occurs with somewhat lower probabilities (calculated by the GEF code [24]) from respective higher excitation energies, which results in more symmetric-like fission. On the contrary, the higher-chance fissions, after emission of several neutrons (3–5, in this case), occur at lower excitation energies, thus they lead predominantly to an asymmetric mass split. The finally calculated FFMD shown by the solid red line is the sum of the FFMDs over the possible multi-chance fissions; it is seen that the measured asymmetric FFMD predominantly comes from the higher-chance fissions. Systematic calculation by extending nuclei and excitation-energies is under way [19].

## 5. Summary and outlook

It is shown that the multi-nucleon transfer reactions are the powerful tool to investigate fission for nuclei which cannot be accessed by particle-capture and heavy-ion fusion reactions. In addition to FFMDs, fission barrier height can be determined. We are also revealing that total spin brought to the fissioning system is nearly proportional to the number of transferred nucleons by measuring the center-of-mass FF angular distributions relative to the rotational axis of CN as an important information for the surrogate reaction technique. Important advantage in the normal kinematics is that the nuclei to be studied can be significantly expanded by using available high-purity radioactive-target. The MNT reactions study using  $^{237}\text{Np}$ ,  $^{234}\text{Am}$ ,  $^{231}\text{Pa}$  and  $^{249}\text{Cf}$  are planned at the JAEA tandem facility. One of the ultimate goal is to use  $^{254}\text{Es}$  target, by which we can study low-energy fissions of fermium

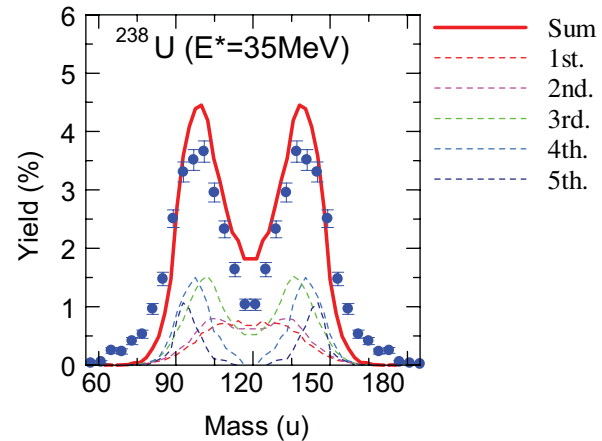


**Figure 7.** Experimental FFMD of  $^{238}\text{U}^*$  (blue symbols) measured at the initial excitation energy of 35 MeV, obtained from the inelastic scattering channel of the reaction  $^{238}\text{U}(^{18}\text{O},^{18}\text{O})^{238}\text{U}^*$ , is compared with the Langevin calculation [20] taking into account multi-chance fission. The solid red curve shows the finally calculated FFMD, where the contributions from every multi-chance fission are shown by the dashed curves with different colors.

isotopes, where sharp transition from the mass-asymmetric fission (e.g.,  $^{256}\text{Fm}$ ) to the sharp symmetric fission (e.g.  $^{258}\text{Fm}$ ) was observed in the spontaneous fission study. Although the available amount of such material could be very limited, the JAEA setup can realize the experiment using only sub- $\mu\text{g}$  material, by taking advantage of the narrow-beam profile ( $\sim 0.5$  mm in diameter) derived from the JAEA tandem accelerator.

In addition to investigate the fission-fragment properties, a measurement of prompt neutrons in coincidence with fission fragments has stated to obtain neutron multiplicity from individual fragment  $\bar{\nu}(A)$  and its excitation energy dependence, by surrounding the fission chamber with 33 liquid-organic scintillation detectors (diameter 12.7 cm  $\times$  thickness 5.1 cm). In the data analysis, neutrons from fissioning nucleus (pre-scission neutron multiplicity  $\nu_{\text{pre}}$ ) and both fragments would be separately obtained by decomposing the energy spectra and angular distribution into three sources.

Special thanks are due to the crew of the JAEA tandem facility for their beam operation. Present study is supported by ‘‘Comprehensive study of delayed-neutron yields for accurate evaluation of kinetics of high-burn up reactors’’ by the Ministry of Education, Culture, Sports, Science and Technology of Japan (MEXT).

## References

- [1] *Nuclear Fission*, R.Vandenbosch and J.R. Huizenga (Academic Press, 1973)
- [2] *Nuclear Fission Process*, edited by C. Wagemans (CRC Press, Boca Raton, FL, 1991)
- [3] K.-H. Schmidt et al., Nucl. Phys. A **665**, 221 (2000)
- [4] G. Boutoux et al., Physics Procedia **47**, 166 (2013)
- [5] A.N. Andreyev et al., Phys. Rev. Lett. **105**, 252502 (2010)
- [6] J.E. Escher et al., Rev. Mod. Phys. **84**, 353 (2012)
- [7] M. Caamaño et al., Phys. Rev. C **88**, 024605 (2013)
- [8] M. Caamaño et al., Phys. Rev. C **92**, 034606 (2015)

- [9] C. Rodríguez-Tajes et al., Phys. Rev. C **89**, 024614 (2014)
- [10] R. LÉguillon et al., Phys. Lett. B **761**, 125 (2016)
- [11] J.F. Siegler, <http://www.srim.org/>
- [12] G. Audi et al., Chinese Physics C **36**, 1287 (2012) and *Ibid.*, M. Wang et al., 1603
- [13] K. Nishio et al., Phys. Rev. C **77**, 064607 (2008)
- [14] V.D. Simutkin et al., Nucl. Data Tables **119**, 331 (2014)
- [15] S.I. Mulgin et al., Nucl. Phys. **A824**, 1 (2009)
- [16] I. Nishinaka, et al., Phys. Rev. C **70**, 014609 (2004) and Proceedings of the Fourth International Conference on Fission and Properties of Neutron-rich Nuclei, Sanibel Island, Florida, USA, 11–17 Nov. 2007, pp. 206–211, World scientific
- [17] I.V. Ryzhov et al., Phys. Rev. C **83**, 054603 (2011)
- [18] Ch. Straede, B. Jørgensen and H.-H. Knitter, Nucl. Phys. **A462**, 85 (1987)
- [19] K. Hirose et al., Preparing for publication
- [20] Y. Aritomo and S. Chiba, Phys. Rev. C **88**, 044614 (2013)
- [21] K. Sato et al., Z. Phys. A **288**, 383 (1978)
- [22] A.N. Ignatyuk et al., Sov. J. Nucl. Phys. **21**, 255 (1975)
- [23] J. Randrup and P. Möller, Phys. Rev. C **88**, 064606 (2013)
- [24] K.-H. Schmidt and B. Jurado and C. Amouroux and C. Schmitt, Nuclear Data Sheets **131**, 107 (2016)